Journal of the European Ceramic Society **15** (1995) 527–535

0955-2219/95/$9.50

0955-2219(95)00014-3

Reactive Formation of Coatings at Boron Carbide Interface with Ti and Cr Powders

P. Mogilevsky,[a] E.Y. Gutmanas,[a]* I. Gotman[b] & R. Telle[c]

[a]Department of Materials Engineering, Technion, Haifa 32000, Israel
[b]Department of Materials Engineering, Drexel University, Philadelphia, PA 19104, USA
[c]Institut für Gesteinshüttenkunde, RWTH, 5-5100 Aachen, Germany

(Received 7 November 1994; revised version received 9 January 1995; accepted 10 January 1995)

Abstract

Boron carbide, B_4C, is an attractive candidate material for reinforcement in metal matrix composites, whose application is severely hampered by its reactions with most engineering alloys at the high processing or service temperatures. The reactivity of B_4C with some of the metals, however, may be made use of to create protective coatings on its surface. In the present research, the microstructure of coatings obtained by the interaction of B_4C with Ti and Cr powders at 1000–1200°C was investigated employing X-ray diffraction, scanning electron microscopy and Auger electron spectroscopy. Coatings obtained by treating B_4C in Ti powder were found to contain Ti carbide, TiC_{1-X}, and Ti borides (TiB_2 and TiB). A relatively thin inner layer of the coating was carbide-free and contained only borides, while the major part of the coating was a mixture of TiC_{1-X} and TiB. In contrast to this, coatings formed by reaction of B_4C with Cr powder contained no carbides, and were shown to consist of Cr borides (CrB_2, CrB, Cr_5B_3 and Cr_2B) and amorphous carbon. A thick outer layer of the coating was carbon-free and consisted almost entirely of CrB. In both cases, the growth of the coatings was controlled by diffusion, the activation energy for the growth of B_4C/Ti coating being approximately 175 KJ/mol. The phase composition, layer sequence and morphology of the coatings obtained were interpreted on the basis of kinetic and thermodynamic data of the ternary systems involved. A good agreement between the experimental results and theoretical predictions was obtained.

1 Introduction

Non-oxide ceramics are important materials having a high potential for advanced structural and electronic applications, as well as reinforcements for metal matrix composites (MMCs). Boron carbide, B_4C, is especially attractive due to its very low density, high hardness and relatively low cost, at least in the particulate form. However, the use of B_4C (as well as other non-oxide ceramics) as a reinforcement for Fe-, Ni- and Co-base alloys is severely hampered by reactions that occur at the ceramic/metal matrix interface at the high processing and/or service temperatures. Although large bulk of evidence exists for the reactivity of non-oxide ceramics with metals,[1–3] the interaction between B_4C and structural Fe-, Ni- and Co-base alloys has practically not been investigated. The solid state reaction between B_4C and nickel at 880°C was reported to yield a complex product at the interface, Ni being a dominant diffusing species.[4] The formation of undesirable reaction products, as well as the dissolution of the ceramic in a metal, result in the degradation of the reinforcement and in the deterioration of the mechanical properties of the matrix and of the MMC as a whole. Since the performance of MMCs is, to a large extent, controlled by the structure and properties of ceramic/metal interfaces, it is important to prevent or, at least, to minimize the reactions at these interfaces. This may be achieved by creating diffusion barriers. The necessity of a diffusion barrier for application of B_4C as a reinforcement for MMCs was emphasized in Ref. 4. One of the possible ways of creating a diffusion barrier is by coating the ceramic prior to inserting it into a metal matrix.

It has been recently shown that non-oxide ceramics such as SiC, Si_3N_4 and B_4C, can be coated employing their interaction with powders of metals having high affinity for carbon, silicon and boron, and a new powder immersion reaction assisted coating method (PIRAC) has been proposed.[5–8] The objective of the present research is to study the microstructure of PIRAC coatings obtained by treating B_4C in Ti and Cr powders.

* To whom correspondence should be addressed.

2 Experimental

In the present research, Cr metal powder (< 150 μm) from Merck, Ti metal powder (~ 100 μm) from Alfa Products and hot pressed boron carbide, B_4C, were used. Plates of B_4C were immersed into the metal powders and heat treated at 1273–1473 K. Heat treatments were conducted in evacuated quartz tubes (10^{-6} Torr at room temperature). After heat treatment, the reacted layers were investigated employing X-ray diffraction, XRD (Philips 1730/10), scanning electron microscopy, SEM, with energy dispersive analysis, EDS (JEOL 840), and Auger electron spectroscopy, AES (Perkin-Elmer PHI 590A).

3 Results and Discussion

3.1 Microstructure of B_4C/Ti powder interface

A representative micrograph of the coating obtained by treating B_4C in Ti powder is shown in Fig. 1. According to the XRD pattern, Fig. 2, the coating consists of a Ti boride, TiB, and the Ti carbide, TiC_{1-X}. The intensities of the TiB peaks do not match the standard intensities, indicating a pronounced (020)-preferred orientation. It should be mentioned that preferred orientation in the direction of the shortest lattice parameter (and [020]/[010] is such a direction for TiB) is often observed during the diffusion growth of compounds with orthorhombic structure.[9] The peaks of TiC_{1-X} are slightly shifted from the standard positions of the stoichiometric TiC, yielding the lattice parameter a ≈ 0·431 nm. This value corresponds to a hypostoichiometric $TiC_{0.6}$ carbide.[10]

Thin coatings obtained after short PIRAC treatments were found to be tightly bonded to the B_4C surface. On the other hand, thicker coatings (> 2–3 μm) tended to spall off the ceramic substrate and stick to the Ti powder, thus revealing the inner surface (coating/B_4C interface) of the reaction layer. A similar behavior was previously observed for PIRAC coatings obtained by treating SiC[7] and Si_3N_4[8] in Ti powder. This allowed to obtain separate AES depth profiles for both the inner, Fig. 3(a), and the outer, Fig. 3(b), layers of the B_4C/Ti coating with good depth resolution. The depth profile in Fig. 3(a) clearly shows that the inner part of the coating is carbon-free and is assumed to be TiB, since this is the only boride detected by XRD. Towards the B_4C surface, however, an increase in the boron content and a corresponding decrease in the Ti content is observed,

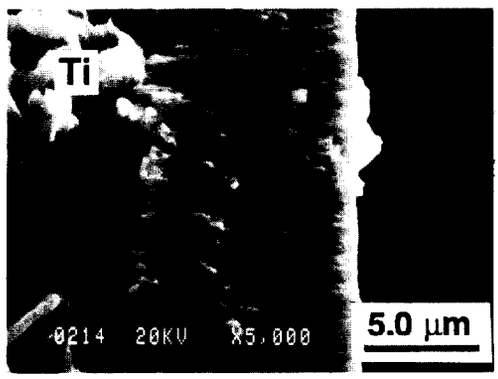

Fig. 1. A representative micrograph of the reaction layer obtained by treating B_4C in Ti powder (1100°C, 6 h), cross section.

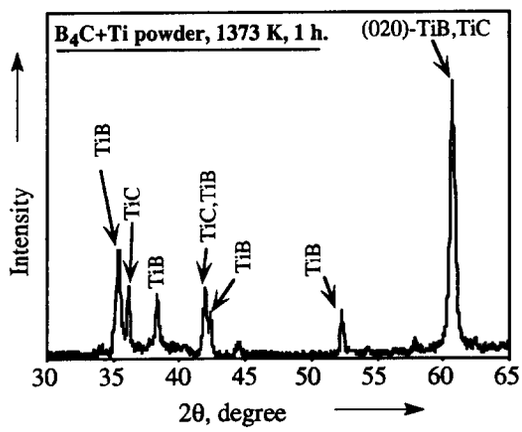

Fig. 2. A typical XRD pattern of the coating obtained by treating B_4C in Ti powder (1100°C, 1 h).

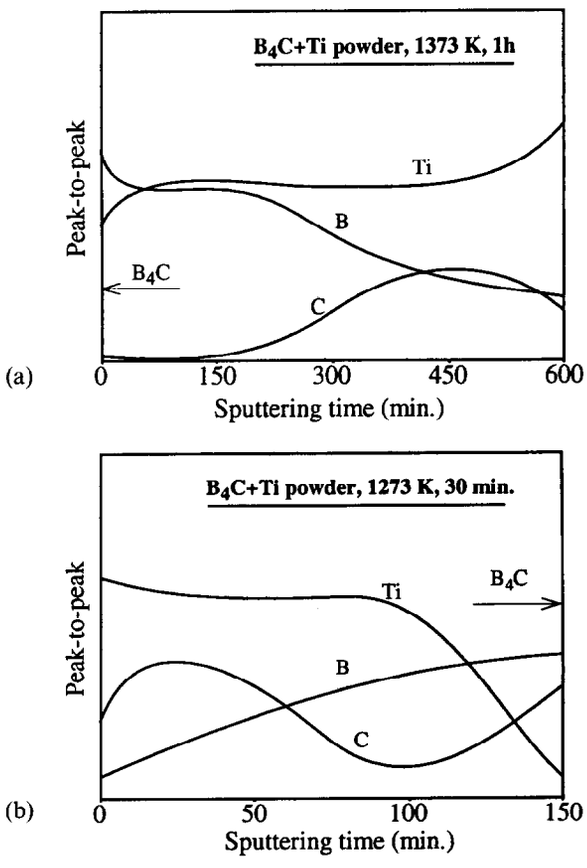

Fig. 3. AES depth profiles of the coatings obtained by treating B_4C in Ti powder: (a) 1100°C, 1 h, sputtering starting from the B_4C/coating interface; (b) 1000°C, 0·5 h, sputtering starting from the coating surface.

Fig. 3(a), suggesting the presence of a thin layer of TiB_2 (or another B-rich boride). Apparently, this layer is too thin to be detected by XRD.

Unlike the inner part of the coating, the outer part contains all the three components — Ti, boron and carbon, Fig. 3(b). It is believed that this part of the coating is a mixture of TiB and TiC_{1-X}, with the amount of TiB gradually decreasing towards the surface. The drop of carbon concentration at the surface of the coating indicates the presence of a layer of TiC_{1-X} with the composition approaching the lower homogeneity limit, i.e. $TiC_{0.5}$. The described sequence of layers in the coating obtained by treating B_4C in Ti powder is schematically shown in Fig. 4.

The results of the kinetic studies, Fig. 5, reveal that the coatings obtained by treating B_4C in Ti powder grow according to the parabolic law, suggesting the diffusion controlled process. The activation energy of growth as calculated from the slope of the Arrhenius plot, Fig. 5(b), is approximately 175 KJ/mol.

In Fig. 6, the diffusion path corresponding to the layer sequence in Fig. 4 is shown superimposed upon the isothermal section of the B–C–Ti system. This diagram has been slightly modified from the one given in[11,12] to reflect the presence of the Ti_3B_4 phase that has been discovered more recently.[13] However, since there is no experimental or theoretical evidence for the stability of this phase at temperatures as low as 1473 K, the Ti_3B_4–TiC_{1-X} tie-line is shown as a dotted line. It can be seen that the experimental results are in a good agreement with the ternary isotherm. The consideration of the diagram shows that TiB_2 is the only phase that forms a stable interface with the stoichiometric B_4C, hence the formation of a thin TiB_2 layer (or TiB_2 and Ti_3B_4 layers) on the B_4C surface. Sections of the diffusion path running along the tie lines from B_4C to TiB_2 and from TiB_2 to TiB are dashed, indicating that B_4C, TiB_2 and TiB single-phase layers are separated by flat interfaces. Similarly, sections of the diffusion path running across a three-phase field to connect a two-phase region to another single-phase region, e.g. (TiB+TiC_{1-X}) to Ti, are drawn with dashed lines, too. This is to indicate that, since no three-phase regions can be formed in course of three component diffusion,[14] the two-phase layer is directly followed (or preceded) by the single-phase layer. (The above comments on the use of dashed lines apply also to the following discussion on the B–C–Cr ternary system). The formation of the

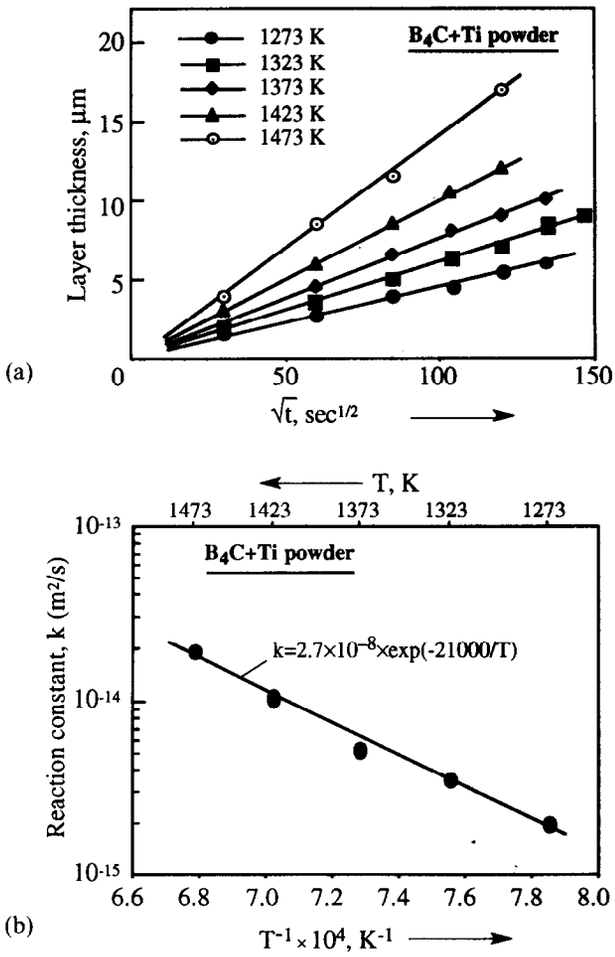

Fig. 5. Kinetics of the coating growth during B_4C/Ti powder interaction: (a) reaction zone thickness versus square root of time at different temperatures; (b) rate of the reaction layer growth versus reciprocal absolute temperature.

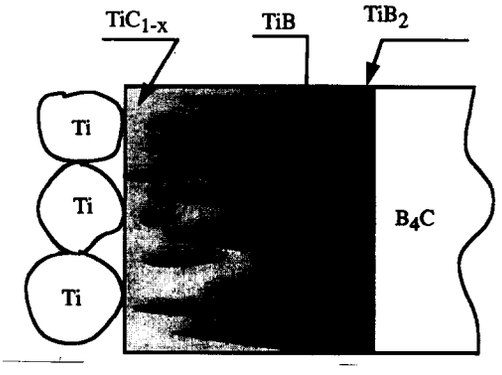

Fig. 4. Schematic of the layer sequence in the B_4C/Ti powder reaction layer obtained at 1000–1200°C.

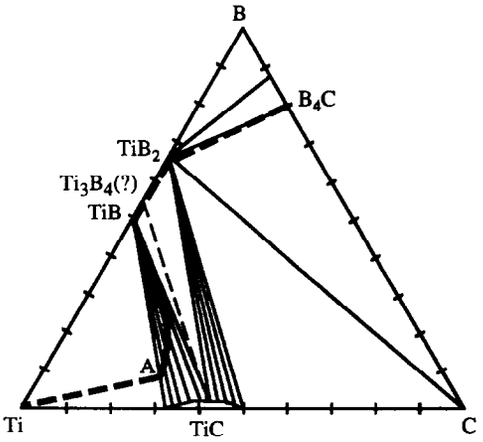

Fig. 6. Isothermal section of the B–C–Ti system at 1500°C.

hypostoichiometric $TiC_{0.6}$ is also in agreement with the diagram, since only a carbon-deficient TiC_{1-x} is in equilibrium with TiB. The same value of (1-x) = 0·6 was obtained by Barsoum *et al.*[15] as the lower limit of (1-x) for TiC_{1-x} in equilibrium with TiB_2 at 1600°C, or, conversely, as the upper limit for TiC_{1-x}in equilibrium with TiB.

In Fig. 6, the major (TiB + TiC_{1-x}) layer of the coating is represented by a section of the diffusion path that passes into a two-phase region (TiB + TiC_{1-x}) from a single phase one (TiB) at an angle to the tie lines and exits into another region. According to Kirkaldy *et al.*,[14] such a diffusion path represents a columnar or a columnar-plus-isolated-precipitate two-phase zone. This suggests that the mixed zone in the B_4C–Ti powder couple contains columnar (and, possibly, some isolated) TiB precipitates in a TiC_{1-x} matrix, the former being rooted in the parent TiB phase, as shown schematically in Fig. 4. Such a microstructure would be consistent both with the observed preferred orientation of TiB, and the columnar-like morphology of the coating cross section, Fig. 1.

The formation of the two-phase (TiB + TiC_{1-x}) layer may be explained by referring to the kinetic model for the formation of an aggregate versus layered morphology in diffusion couples, suggested by Rapp *et al.*[16] Although developed for less complicated diffusion layer sequences, the model seems to be well applicable to our B_4C/Ti powder system. If an initially planar interface between the TiB and TiC_{1-x} layers is assumed, the model predicts[16,17] that it will remain flat provided the growth of the TiB layer is limited by B diffusion through TiB. Alternatively, if the diffusion of Ti through TiC_{1-x} is the rate-limiting step, the two-phase aggregate morphology will result. In our case, the growth of TiB is, most probably, limited by Ti diffusion (the mobile B atoms usually diffuse much faster than the Ti atoms), hence the formation of the two-phase (TiB + TiC_{1-x}) layer in the coating, Fig. 4. Another comment that can be made regarding the relative diffusion rates in the B_4C/Ti couple is that, since the TiC_{1-x} carbide constitutes the major part of the foremost layer of the coating leaving behind the TiB boride, the diffusion of carbon in TiB must be more rapid than that of boron.

3.2 Microstructure of B_4C/Cr powder interface

A representative microstructure of the coating obtained by treating B_4C in Cr powder is shown in Fig. 7. In the micrograph, two morphologically different layers can be distinguished, the outer one having a pronounced 'columnar' structure. Coatings obtained after 1 – 4 h exposures at 1200°C were approximately 14 – 18 μm thick, and they

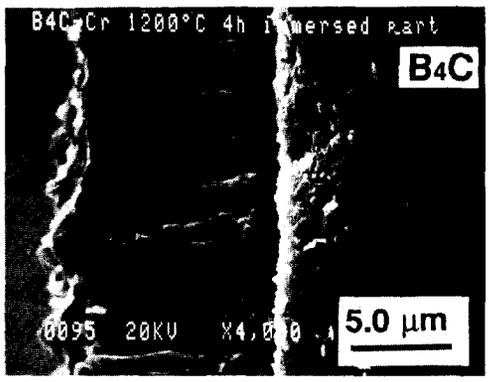

Fig. 7. A representative micrograph of the reaction layer obtained by treating B_4C in Cr powder (1200°C, 4 h), cross section.

easily split (e.g. during polishing) along the sublayer interface. A layer of carbon black was detected on both fracture surfaces. On the other hand, no splitting was observed in the thinner coatings (~7 μm) formed during 0·5 h exposure at 1100°C.

In Fig. 8(a), a typical XRD pattern of the coatings obtained at 1100–1200°C is presented. It can be seen that the coatings consist of different Cr borides: CrB as a major phase, Cr_5B_3 and Cr_2B. The pronounced (002) orientation of CrB suggests that this boride constitutes the outer layer of the

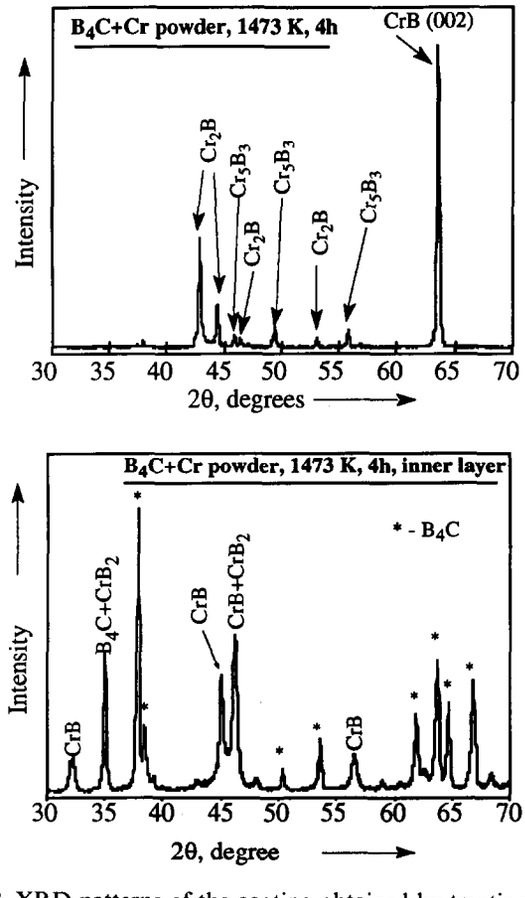

Fig. 8. XRD patterns of the coating obtained by treating B_4C in Cr powder (1200°C, 4 h): (a) the entire coating; (b) the inner layer.

coating having the 'columnar' morphology, Fig. 7. Similarly to the case of TiB, the preferred orientation is in the direction of the orthorhombic unit cell shortest parameter—[002]/[001] for the CrB lattice. The splitting of the coatings obtained at 1200°C made it possible to remove the outer layer and identify the phase composition of the inner layer more accurately. According to the XRD pattern in Fig. 8(b), the inner layer of the coatings obtained at 1200°C consists of CrB (with no preferred orientation) and CrB_2 (It should be mentioned that the XRD detection of CrB_2 is not unequivocal due to the superposition of the lines of CrB_2 and CrB or B_4C. However, the anomalously high intensity of the CrB peak at around $2\theta = 46°$ gives ground to the suggestion that the peak is, in fact, a superposition of the CrB (I/I_{max} = 80%) and CrB_2 (I/I_{max} = 100%) peaks. An alternative assumption that the high intensity of the peak is a result of a certain preferred orientation of CrB is not corroborated by other CrB peak intensities.) Since the coating obtained at 1100°C did not split, no separate XRD analysis of the inner layer phase composition was made. The XRD pattern of the coating as a whole does not indicate the presence of CrB_2 observed in the inner layer of the coating obtained at 1200°C.

The striking feature of the XRD results is the absence of Cr carbides or any other carbon-containing phases including graphite. It is clear, however, that since carbon is one of the products of B_4C decomposition, it should be present in the coating in some form. Indeed, a typical AES depth profile in Fig. 9(a) (1200°C, 4 h) shows that the inner layer of the coating contains, in addition to B and Cr, a large and constant amount of carbon. This mixed C–B–Cr layer is followed by a thin sublayer of pure carbon apparently corresponding to the 'split plane' of the coating. (It should be mentioned, that AES profiling to such a depth (~14 μm) was only made possible due to the splitting of the coating. In fact, three separate depth profiles were obtained: one from the surface of the coating, and two from each 'split surface'. The profile in Fig. 9(a) is a reconstruction based on the three above profiles.) The shape of the carbon KVV-peak in the AES spectrum, Fig. 9(b), was found to match that of the free rather than bound (carbide) carbon.[18] Since no graphite peaks were observed in the XRD pattern, the carbon in the coating is assumed to be amorphous. The profile in Fig. 9(a) clearly shows that the outer layer of the coating is carbon-free thus confirming our early assumption that this is a pure CrB layer. The increase of Cr concentration towards the surface of the coating, coupled with the XRD results, Fig. 8(a) suggests the presence of thin Cr_5B_3 and Cr_2B surface sublayers.

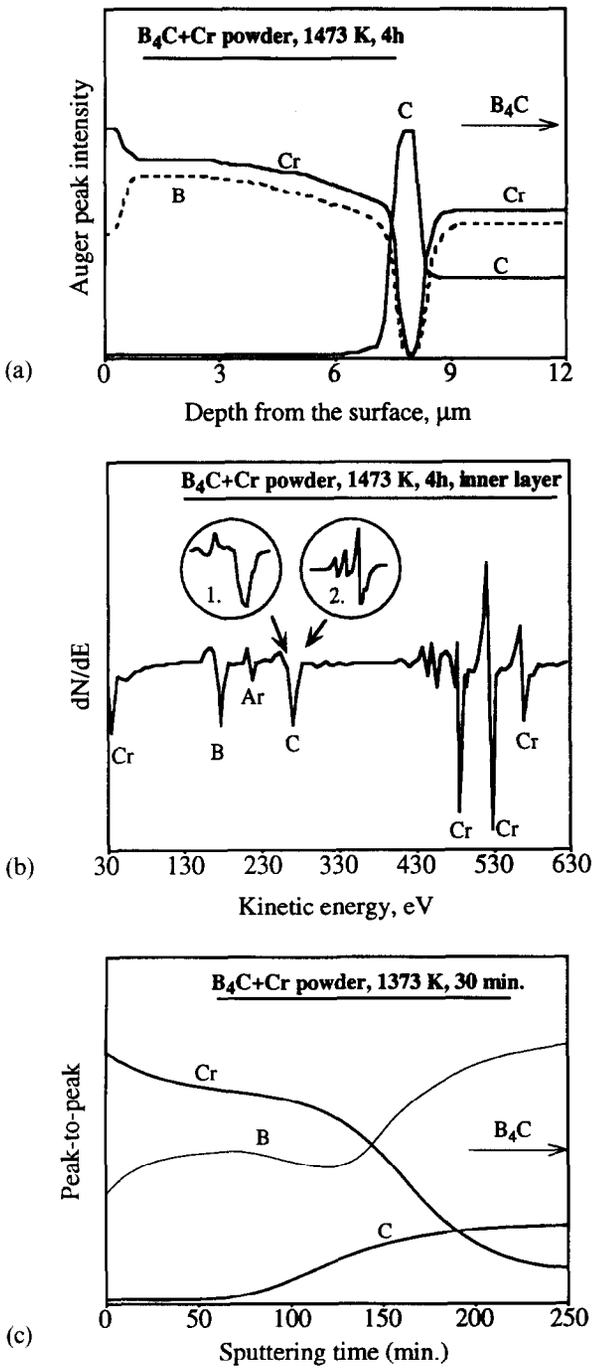

Fig. 9. AES results for the coatings obtained by treating B_4C in Cr powder: (a) 1200°C, 4 h, reconstructed depth profile, depth scale given according to SEM thickness; (b) 1200°C, 4 h, spectrum from the inner layer: 1 — KVV peak of free (unbound) carbon, 2 — KVV peak of bound (carbide) carbon; (c) 1100°C, 0·5 h, depth profile.

AES depth profile of the coating obtained at 1373 K, Fig. 9(c), being in all other respects similar to that in Fig. 9(a), does not reveal the presence of the pure carbon sublayer. This is consistent with the observation that these coatings do not split along the sublayer interface. It should be mentioned, however, that the inability to detect a thin carbon layer may also be the result of an insufficient depth resolution.

Based on the above observations, the sequences of layers in the coatings obtained by treating B_4C in Cr powder at 1100 and 1200°C were suggested

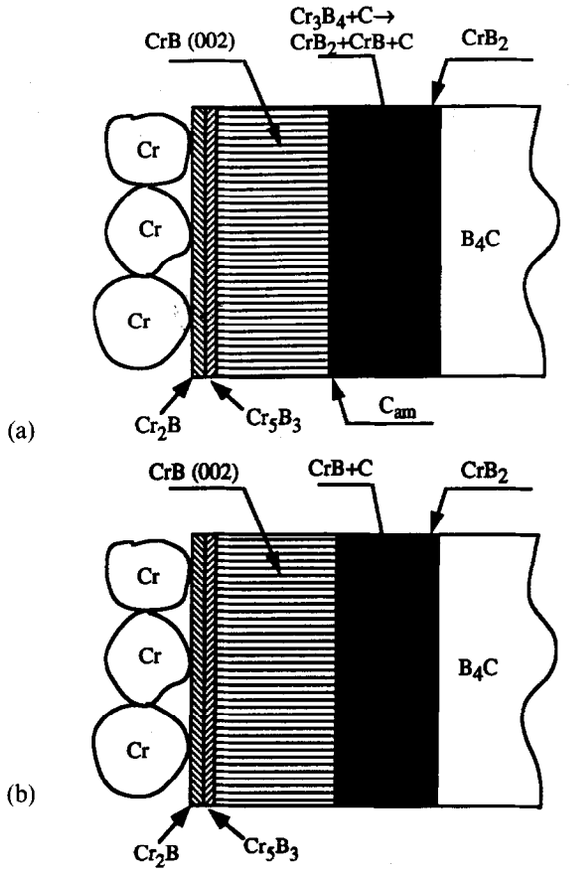

Fig. 10. Schematics of the layer sequences in the coatings obtained by treating B_4C in Cr powder at: (a) 1200°C; (b) 1100°C.

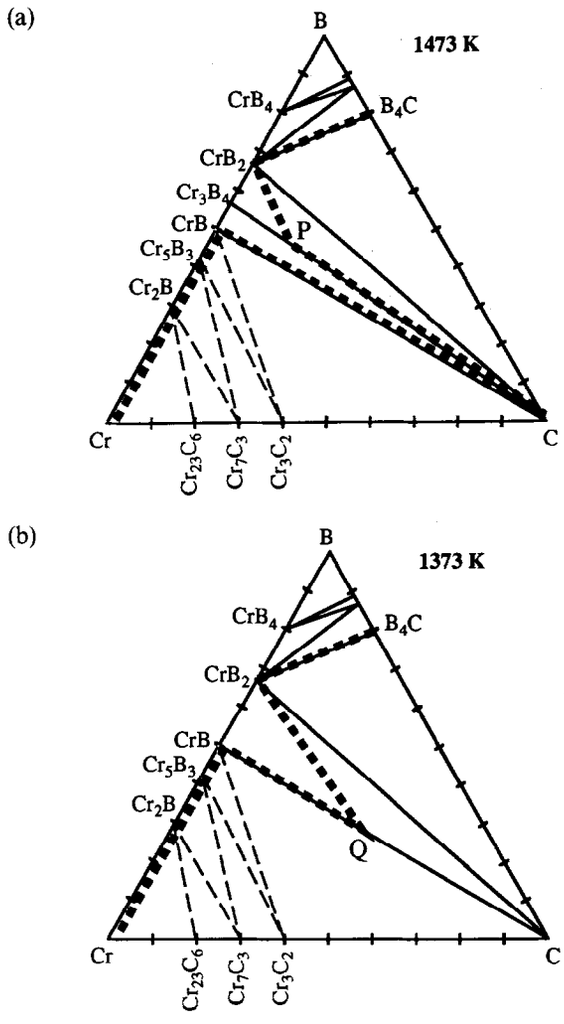

Fig. 11. Tentative isothermal sections of the B–C–Cr system at: (a) 1200°C; (b) 1100°C.

and are shown schematically in Figs. 10(a) and (b), respectively. It can be seen that for the coating obtained at 1200°C, Fig. 10(a), the inner layer containing amorphous carbon, CrB and a small amount of CrB_2, is followed by a thin sublayer of pure carbon black which is, in turn, followed by a layer of columnar (002) oriented CrB grains. Towards the surface of the coating, CrB gives way to the thin sublayers of Cr-rich borides Cr_5B_3 and Cr_2B. For the coating obtained at 1100°C, Fig. 10(b), we assume the inner layer to be a mixture of amorphous carbon and CrB only (since no indication as to the presence of CrB_2 was obtained). The outer carbon-free layer of the coating obtained at 1100°C is similar to that of the 1200°C coating; however, no intermediate sublayer of carbon black is observed in the former.

As seen from Fig. 10, the coatings obtained have rather complex microstructures. Thus, it would be very interesting to try and superimpose the diffusion paths corresponding to the observed phase sequences onto the B–C–Cr ternary diagram. (The 'diffusion path' approach is justified, since the coatings growth in the B_4C–Cr powder system was earlier reported[6] to be controlled by diffusion.) Unfortunately, no isothermal sections of either complete B–C–Cr ternary diagram, or of its B- and C-rich corners are available in the literature. In order to make the discussion of our results possible, an attempt was made to construct tentative isothermal 1100 and 1200°C sections of the B–C–Cr diagram, based on the available literature data as well as on our own experimental results. The tentative isothermal sections are shown in Fig. 11, and they are based on the following assumptions:

- B–C–Cr ternary diagram is, in general, similar to the B–C–Mo[12] and B–C–W[11,12] ternaries, since Cr, Mo and W are transition metals belonging to the same group of the periodic table;
- CrB and CrB_2 are at equilibrium with carbon at temperatures above 1350°C.[19,20] If we assume that the equilibrium pertains to the lower temperatures (down to 1100°C), there are CrB–C and CrB_2–C tie lines on the B–C–Cr ternary isotherms at both 1100 and 1200°C;
- CrB_2 is at equilibrium with B_4C up to 2100°C,[19] i.e. there is a B_4C–CrB_2 tie line on the B–C–Cr ternary isotherms at both 1100 and 1200°C;

- Cr_3B_4 is unstable at temperatures below ~1200°C, and it decomposes at 1100°C < T < 1200°C according to $Cr_3B_4 \rightarrow 2CrB + CrB_2$, similarly to the decomposition of MoB_2 into MoB and Mo_2B_5 at ~1480°C.[21] To establish this, and elemental Cr/B powder blend with the composition corresponding to Cr_3B_4 was compacted, heat treated and analyzed by XRD. The only phase found in the compact annealed at 1200°C for 4 h and rapidly cooled to the room temperature was Cr_3B_4. On the other hand, only traces of Cr_3B_4 were found in the sample slowly cooled from the same temperature, the main peaks being those of CrB and CrB_2. Similarly, the compacts annealed at 1100°C, both rapidly and slowly cooled, consisted of CrB and CrB_2 phases, only. These results suggest that Cr_3B_4 is thermodynamically stable at 1200°C, but is not stable at 1100°C. Therefore, the Cr_3B_4 boride is present in the B–C–Cr ternary isotherm at 1200°C, but it is absent at 1100°C.

Since the Cr-rich corner of the B–C–Cr ternary is very complicated and as it is not this part of the diagram that we're concerned about, its presentation in Fig. 11 is rather simplified (hence the use of dashed lines). An accurate representation of the Cr-rich corner may be found in Ref. 22.

The diffusion paths mapped onto the ternary isotherms in Fig. 11 correspond to the layer sequences shown in Fig. 10. The existence of the CrB_2 – C tie line makes the equilibrium between B_4C and CrB impossible and thus requires the presence of CrB_2 at the B_4C/coating interface. We assume, therefore, that there is a thin interfacial CrB_2 sublayer in the coatings obtained at both 1100 and 1200°C. The layer must be so thin that it could not be detected by XRD, at least for the 1100°C coating. AES depth profiling also proved ineffective in revealing this thin CrB_2 sublayer, apparently as a result of the poor depth resolution in the vicinity of the deeply buried (~7 μm for the 1100°C coating) B_4C/coating interface. (It is worth mentioning, that the detection by AES of the similar TiB_2 sublayer at the B_4C/Ti-base coating, Fig. 3(a), was only made possible due to the spalling of the coating off the ceramic substrate along the B_4C/TiB_2 interface.)

With the above considerations in mind, one can see that the diffusion path in Fig. 11(b) closely follows the layer sequence observed in the coating formed at 1100°C, Fig. 10(b). This is also the case for the coating obtained at 1200°C, with one exception, however. Namely, the diffusion path depicted in Fig. 11(a) requires the presence of a (Cr_3B_4 + carbon) two-phase layer preceding the pure carbon layer, whereas, in the real coating, the (CrB + CrB_2 + carbon) layer is observed, Fig. 10(a). It is apparent that such a three-phase layer could not be formed in our three component system during the process of diffusion growth. This discrepancy can easily be explained by the already mentioned decomposition of Cr_3B_4 at temperatures below 1200°C. We believe that a (Cr_3B_4 + carbon) layer is actually formed at the processing temperature of 1200°C, and is subsequently transformed into the experimentally observed (CrB + CrB_2 + carbon) layer on cooling to the room temperature. Since the exact compositions of the (CrB + CrB_2 + carbon) layer in the 1200°C coating and of the (CrB + carbon) layer in the 1100°C coating have not been measured, the points P and Q representing these layers on the ternary isotherms, Figs. 11(a) and (b), respectively, are given just as a reference.

The formation of the two-phase (Cr_3B_4 + carbon) layer versus the flat carbon/CrB interface in the 1200°C coating is in an agreement with the kinetic model[16] referred to in the previous section. The model predicts that, assuming initially planar interfaces and Cr diffusion as the rate-determining step (that is justified considering the much higher mobility of carbon and boron atoms), the aggregate morphology should develop at the Cr_3B_4/carbon interface yielding the two-phase (Cr_3B_4 + carbon) region, whereas the layered morphology should be preserved at the carbon/CrB interface. These are the morphologies experimentally observed in our diffusion couple, Fig. 10. On the other hand, the attempt to apply the model to the 1100°C coating morphology proved unsuccessful. A more thorough investigation of the microstructure of the coatings obtained by treating B_4C in Cr powder at 1100°C is now in progress. An interesting observation regarding the coatings in the B_4C/Cr powder system is that thick carbon-free pure boride (CrB) surface layers are formed. This suggests that, in contrast to the B_4C/Ti coatings, the diffusion of boron through the reaction products is faster than that of carbon.

4 Summary and Conclusions

It was shown that the interaction of B_4C with Ti and Cr powders at 1000–1200°C yielded complex multi-layer coatings on the ceramic substrate. Coatings obtained by treating B_4C in Ti powder were found to contain the Ti carbide, TiC_{1-X}, and Ti borides (TiB_2, TiB). A relatively thin inner layer of the coating was carbide-free and contained only borides, while the major part of the

coating was a mixture of TiC_{1-X} and TiB. In contrast to this, coatings formed by reaction of B_4C with Cr powder contained no carbides, and were shown to consist of Cr borides (CrB_2, CrB, Cr_5B_3 and Cr_2B) and amorphous carbon. A thick outer layer of the coating was carbon-free and consisted almost entirely of CrB. In both cases, the growth of the PIRAC coatings was controlled by diffusion. The activation energy for the growth of B_4C/Ti coating was found to be approximately 175 Kj/mol. The phase composition and the layer sequences in the coatings obtained were analyzed by mapping the diffusion paths onto the corresponding ternary isotherms. Since no B–C–Cr phase diagram was available in literature, tentative B–C–Cr ternary isotherms were proposed for the temperatures of 1100 and 1200°C. The layer sequence and morphology of the PIRAC coatings were interpreted also on a kinetic basis. The experimental results were found to be in a fair agreement with the kinetic and thermodynamic predictions for the ternary systems involved.

Once PIRAC has been proved useful for coating B_4C ceramic, the next question to be answered is whether the coatings obtained are feasible as protective layers at various B_4C/metal interfaces. To be effective, these coatings should act as diffusion barriers as well as be sufficiently inert with respect to the metal. In addition, thermal expansion coefficients (CTE) of B_4C, the metal and the coating should be considered. Due to the complex structure of the coatings obtained, as well as to the lack of essential data on the diffusion of metals, carbon and boron in borides and carbides and their CTE's, theoretical predictions of the coatings integrity as protective layers are hard to make. Preliminary results have shown that both the Ti- and Cr-based PIRAC coating effectively suppress the interaction of B_4C with iron at 1000–1100°C.[6] Clearly, only relatively thin reaction layers that do not spall off the B_4C surface can be considered as candidates for protective coatings. It would be especially interesting to study the effect of the pure carbon and the mixed carbon/CrB layers on the protective behavior of Cr-based PIRAC coatings on B_4C surface. Carbon coatings are now routinely used as protective layers on SiC fibers (e.g. SCS-6 Textron-AVCO SiC fibers). It should be mentioned, however, that if B_4C-particulate reinforced MMCs (e.g. for wear applications) are considered, the low strength of a pure carbon layer may have an adverse effect on the bonding integrity of B_4C particles in a metal matrix. Further investigation of the coatings' behavior in different metal matrices is required to find out whether they can act as adequate protective layers at B_4C/metal interfaces.

Acknowledgements

The authors would like to thank Dr R. Brener for performing the Auger analysis. This research was supported by G.I.F. Research Grant No. 10069-326.10.87.

References

1. Brito, M. E., Matsumoto, J. M., Hirótusu, Y., Fukuzawa, Y. & Tanaka, K., Solid state reaction of nickel on silicon carbide. In *Joining Ceramics, Glass and Metal*, ed. W. Kraft. DGM Informationgesellshaft, 1984, pp. 305–12.
2. Klomp, J. T., Thermodynamics of ceramic–metal interfaces. In *Designing Interfaces for Technological Applications: Ceramic–Ceramic, Ceramic–Metal Joining*, ed. S. D. Peteves. Elsevier, London, 1989, pp. 127–44.
3. Backhaus-Ricoult, M., Physicochemical processes at metal–ceramic interfaces. In *Designing Interfaces for Technological Applications: Ceramic–Ceramic, Ceramic–Metal Joining*, ed. S. D. Peteves. Elsevier, London, 1989, pp. 79–92.
4. Yang, J. -M., Kao, W. H., & Liu, C. T., Interface characterization of fiber-reinforced Ni_3Al matrix composites, *Metall. Trans.*, **A20** (1989) 2459–69.
5. Gutmanas, E. Y, Gotman, I. & Kaysser, W., Coating of non-oxide ceramics by interaction with metal powders. *Mater. Sci. Eng.*, **A157** (1992) 233–41.
6. Mogilevsky, P., Gotman, I., Gutmanas, E. Y. & Kaysser, W., Microstructure and thermal stability of coatings obtained by interaction of SiC and B_4C with Cr and Ti powders. *Mater. Sci. Eng.*, **A170** (1993) 271–9.
7. Gotman, I., Gutmanas, E. Y. & Mogilevsky, P., Interaction between SiC and Ti powder. *Mater. Res.*, **8** (1993) 2725–33.
8. Gotman, I., Interaction of SiC and Si_3N_4 with metal powders. PhD Thesis, Technion — Israel Institute of Technology, Haifa, Israel, 1991.
9. Van Loo, F. J. J., Multiphase diffusion in binary and ternary solid-state systems. *Prog. Solid St. Chem.*, **20** (1990) 47–99.
10. Kosolapova, T. Ya., *Carbides*. Plenum Press, New York, 1971, p. 98.
11. Rudy, E., *Ternary Phase Equilibria in Transition Metal Boron–Carbon–Silicon Systems*, Part V, Report No. AFML-TR-65-2. Air Force Materials Laboratory, Ohio, 1969, p. 606.
12. Schouler, M., Ducarroir, M. & Bernard, C., Review on constitution and properties of the metal–carbon–nitrogen and metal–carbon–boron systems. *Rev. Int. Hautes Temp. Réfract.*, **20** (1983) 261–311.
13. Spear, K. E., McDowell, P. & MeMahon, F., Experimental evidence for the existence of the Ti_3B_4 phase. *J. Am. Ceram. Soc.*, **69** (1986) C-4 – 5.
14. Kirkaldy, J. S. & Young, D. J., *Diffusion in the Condensed State*. The Institute of Metals, London, England, 1987, pp. 361–99.
15. Barsoum, M. & Houng, B., Transient plastic phase processing of titanium–boron–carbon composites. *J. Am. Ceram. Soc.*, **76** (1993) 1445–51.
16. Rapp, R. A., Ezis, A. & Yurek, G., Displacement reactions in the solid state. *Metall. Trans.*, **4** (1973) 1283–92.
17. Van Loo, F. J. J., van Beek, J. A., Bastin, G. F. & Metselaar, R., The role of thermodynamics and kinetics in multiphase ternary diffusion. In *Diffusion in Solids*, eds. M. A. Dayananda & G. E. Murch. TMS, Warrendale, 1985, pp. 231-59.

18. H. E. Bishop, Auger electron spectroscopy. In *Methods of Surface Analysis*, ed. J. M. Walls. Cambridge University Press, Cambridge, England, 1989, pp. 87–126.
19. Glaser, F. W., Contribution to the metal–carbon–boron systems. Trans. AIME, **194** (1952) 391–6.
20. Markovskii, L. Ya., Vekshina, N. V. & Bezruk, E. T., Interaction of borides with carbon and carbides. In *Chemical Properties and Analysis of Refractory Compounds*, ed. G. V. Samsonov. Consultants Bureau, New York – London, 1972, pp. 114–17.
21. Portnoi, K. I. & Romashov, V. M., Binary constitution diagrams of systems composed of various elements and boron — A review. *Sov. Powder Met. Ceram.*, **11** (1972) 378–84.
22. Pradelli, G., Research on chromium borocarbides. *Met Ital.*, **66** (1974) 551–6.